

CASE REPORT

Open Access



A primary intracranial neuroepithelial neoplasm with novel *TCF3::BEND2* fusion: a case report

Linmao Zheng^{1,2}, Tao Luo³, Jie Xian^{1,2}, Mengxin Zhang^{1,2}, Xiuyi Pan^{1,2}, Xiang Wang⁴, Qiang Yue⁵, Qiao Zhou^{1,2} and Ni Chen^{1,2*}

Abstract

Astroblastoma, *MN1*-altered, is a rare circumscribed glial neoplasm that is composed of round, cuboidal, or columnar cells with astroblastic perivascular pseudorosettes, often associated with *MN1::BEND2* and *MN1::CXXC5* fusions. Atroblastoma-like gliomas harbouring *EWSR1::BEND2* have been reported that they defined an epigenetically distinct subtype of astroblastoma. We report a case of a 19-year-old female with an intracranial neuroepithelial tumor featuring a novel *TCF3::BEND2* fusion. This tumor, while classified as *EWSR1::BEND2* gliomas based on DNA methylation, did not exhibit the *MN1* alteration or typical astroblastoma morphology. The patient, initially diagnosed as ependymoma WHO grade 2 following surgery for an intracranial tumor four years prior, presented with a suspected recurrence. Magnetic resonance imaging identified a mixed solid-cystic lesion in the temporal area of the left lateral ventricle. For the recurrent tumor, the histological examination revealed the tumor cells predominantly exhibited a solid arrangement, with the solid areas primarily consisting of oval and short-spindle cells. In certain regions, loosely arranged short-spindle cells were observed. The tumor exhibited high cellular density, nuclear atypia, and frequent mitoses, but lacked the hallmark features typically associated with astroblastoma. Immunohistochemistry revealed patchy positivity for GFAP and OLIG2, diffuse positivity for EMA, and a high MIB-1 labeling index. Genome-wide DNA methylation profiling confirmed the tumor's classification as *EWSR1::BEND2* gliomas with a high-confidence match and revealed focal deletion of chromosome 9q. Targeted next-generation sequencing identified a *TCF3::BEND2* fusion, validated by reverse transcription polymerase chain reaction and Sanger sequencing. This case broadens the genetic spectrum of high-grade neuroepithelial tumor and suggests that *BEND2* alterations may serve as critical determinants for this *EWSR1::BEND2* glioma subgroup within the methylation classifier.

Keywords Brain tumor, HGNET, DNA methylation, *TCF3*, *BEND2*

*Correspondence:

Ni Chen
chenni1@163.com

¹Department of Pathology, West China Hospital, Sichuan University, Chengdu, Sichuan 610041, China

²Laboratory of Pathology, West China Hospital, Sichuan University, Chengdu, Sichuan, China

³Institute of Pathology, Southwest Hospital, Third Military Medical University (Army Medical University), Chongqing, China

⁴Department of Neurosurgery, West China Hospital, Sichuan University, Chengdu, China

⁵Department of Radiology, West China Hospital of Sichuan University, Chengdu, China



Introduction

Astroblastoma, *MN1*-altered, is a rare circumscribed glial neoplasm that is composed of round, cuboidal, or columnar cells with astroblastic perivascular pseudorosettes, often associated with *MN1::BEN Domain Containing 2 (BEND2)* and *MN1::CXXC-type zinc finger protein 5 (CXXC5)* fusions and primarily occur in the cerebral hemisphere [1]. *MN1::BEND2* fusion is the most common fusion in astroblastoma with *MN1* alteration [2]. *Ewing sarcoma RNA-binding protein 1 (EWSR1)::BEND2* glioma is a type of tumor exhibiting morphological features of astroblastoma characterized by *EWSR1::BEND2* fusion. It has been reported that *EWSR1::BEND2* gliomas defined an epigenetically distinct subtype of astroblastoma, mostly in the spinal cord [3, 4]. Herein, we report a primary intracranial neuroepithelial neoplasm with a novel *Transcription Factor 3 (TCF3)::BEND2* fusion. It was classified as *EWSR1::BEND2* gliomas based on DNA methylation but lacked the typical astroblastoma morphology.

Case presentation

A 19-year-old female patient, who underwent intracranial tumor surgery at an outside hospital four years ago (August 2019), was admitted to our hospital in May 2023 for a suspected recurrent intracranial tumor. Magnetic resonance imaging revealed a 5.7 cm x 5.3 cm x 4.8 cm mixed solid-cystic lesion centered in the temporal area of the left lateral ventricle (Fig. 1A-D). No other lesions were identified. The initial postoperative pathological diagnosis for the patient was ependymoma, WHO grade 2. The tumor had well-demarcated borders with the surrounding tissue. Most tumor cells were arranged in a rosette-like pattern, with a collagenous fibrous stroma, resembling an astroblastoma. In some areas, the tumor cells were arranged in solid sheets. Nuclear grooves were observed in some of the tumor cells (Fig. 2). The patient passed away one year after the second surgery in May 2024. The patient did not undergo any radiotherapy or chemotherapy. The patient's progression-free survival (PFS) was 44 months, and overall survival (OS) was 56 months.

Histological examination (Fig. 3) revealed that the recurrent tumor cells predominantly exhibited a solid arrangement, with the solid areas primarily consisting of oval and short-spindle cells. In certain regions, loosely

arranged short-spindle cells were observed with a mucinous background noted. Additionally, isolated areas displayed pseudorosettes structures formed by epithelial cells. The tumor had a high cellular density, with some exhibiting significant nuclear atypia and visible nuclear grooves, and frequent mitoses. Areas of coagulative necrosis were observed, with a few perivascular pseudorosettes at the margins. Typical astroblastoma-like pseudorosettes or sclerotic stroma were absent.

Immunohistochemically, the tumor cells showed patchy expression of GFAP (Fig. 4A), OLIG2 (Fig. 4B), NSE and NESTIN, diffusely positive for CD56, D2-40, EMA (Fig. 4C), H3K27me3, SOX2 (Fig. 4D), SOX9 and p16 (Fig. 4E), negative for ALK-1, CD1a, CD30, CD34, CD99, CD163, Desmin, L1CAM, PCK, PR, pTRK, S-100, SOX10, SSTR2, STAT6, Syn. The MIB-1 labelling was 40% (Fig. 4F). Reticulin staining revealed a paucity of reticulin fibers.

DNA methylation array analysis was conducted using R version 4.1.0, with the minfi package (version 1.40.0) from Bioconductor (version 3.14) [5] to extract raw signal intensities from the IDAT files of the methylation arrays. The data were normalized using the preprocess Quantile function. Methylation sites on the X and Y chromosomes were excluded, as well as non-informative sites from the 450 K array. The top 20,000 most variable methylation sites were selected for clustering analysis. Two clustering methods were applied: the t-distributed stochastic neighbor embedding (t-SNE) method, implemented using the Rtsne package, and the Uniform Manifold Approximation and Projection (UMAP) method, performed with the UMAP package. In the clustering analysis shown in Fig. 5, the present case was positioned in close proximity to the *EWSR1::BEND2* gliomas group across both t-SNE (Fig. 5A) and UMAP plots (Fig. 5B), suggesting a strong similarity in methylation profiles between the present case and the *EWSR1::BEND2* glioma subtype. Unsupervised hierarchical clustering pattern highlighted a potential relationship between the present case and *EWSR1::BEND2* gliomas (Fig. 5C), implying that the case may share molecular characteristics with this *EWSR1::BEND2* glioma subtype. Hypermethylation of the *O⁶-methylguanine methyl transferase (MGMT)* gene promoter was absent. Chromosomal copy number analysis from DNA methylation arrays showed focal deletion of chromosome 9q (Fig. 6A).

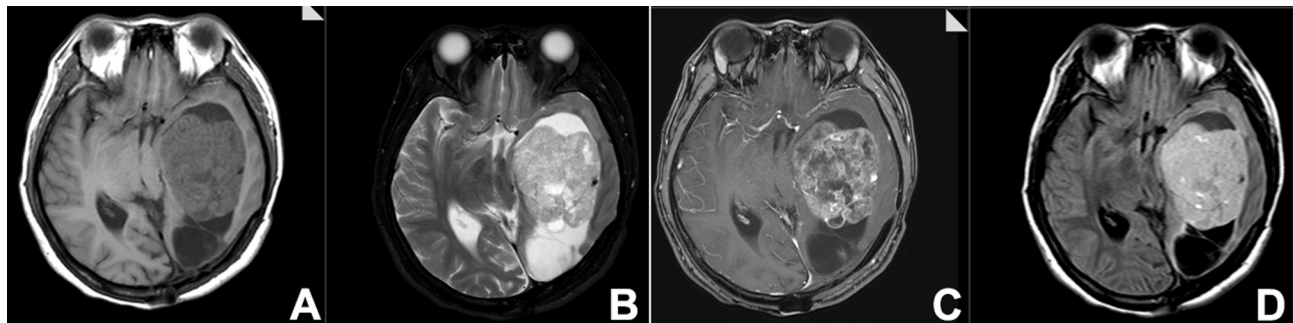


Fig. 1 MRI showed a mixed solid-cystic lesion centered in the temporal area of the left lateral ventricle, low signal intensity on T1-weighted images (**A**) and high signal intensity on T2-weighted images (**B**). Fluid attenuated inversion recovery (FLAIR) images showed the mass to be primarily hyperintense (**C**). Contrast-enhanced imaging demonstrated marked, heterogeneous enhancement within the lesion, with the presence of tortuous and enlarged blood vessels (**D**)

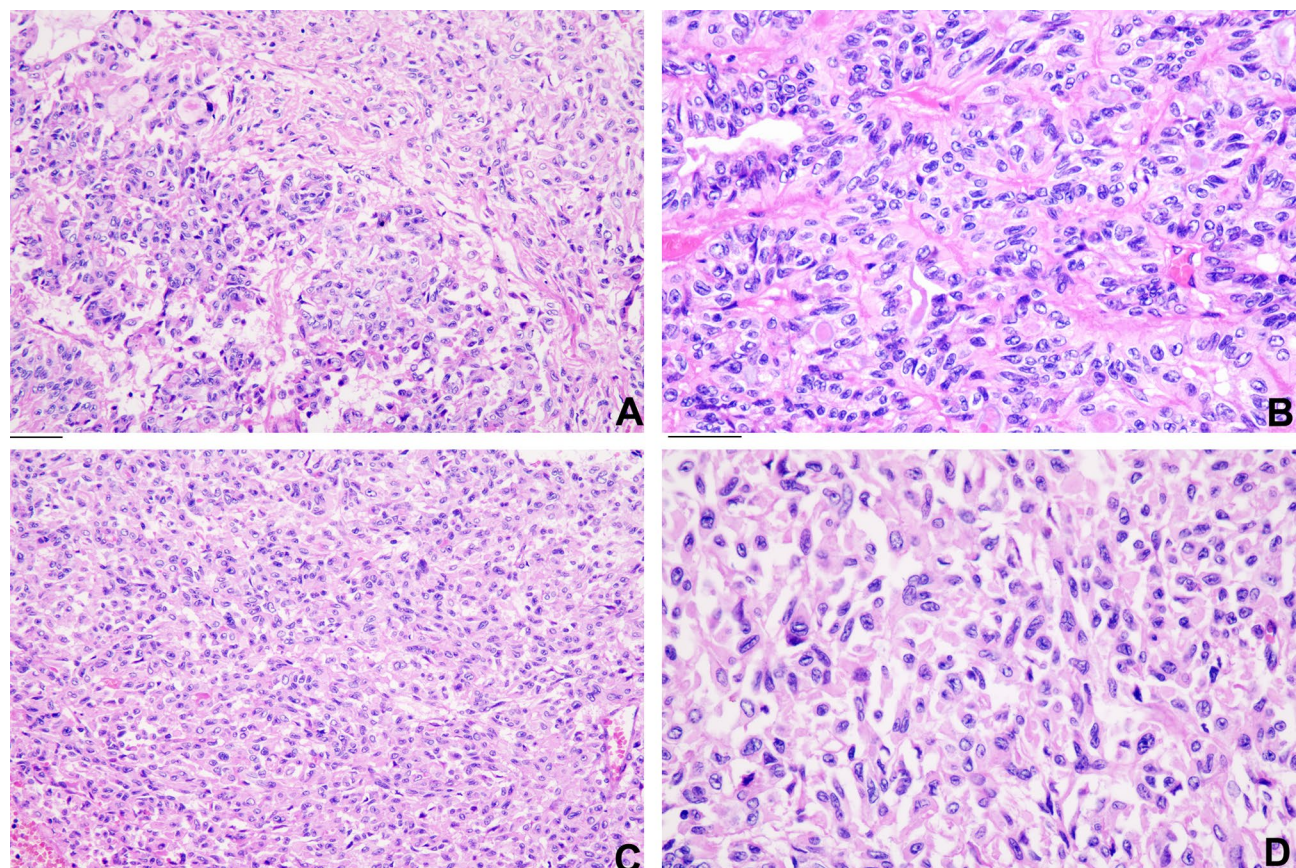


Fig. 2 Histopathological features of the initial tumor. Most tumor cells were arranged in a rosette-like pattern (A, B), with a collagenous fibrous stroma (B). In some areas, the tumor cells were arranged in solid sheets (C). Nuclear grooves were observed in some of the tumor cells (D). (bar = 50 µm)

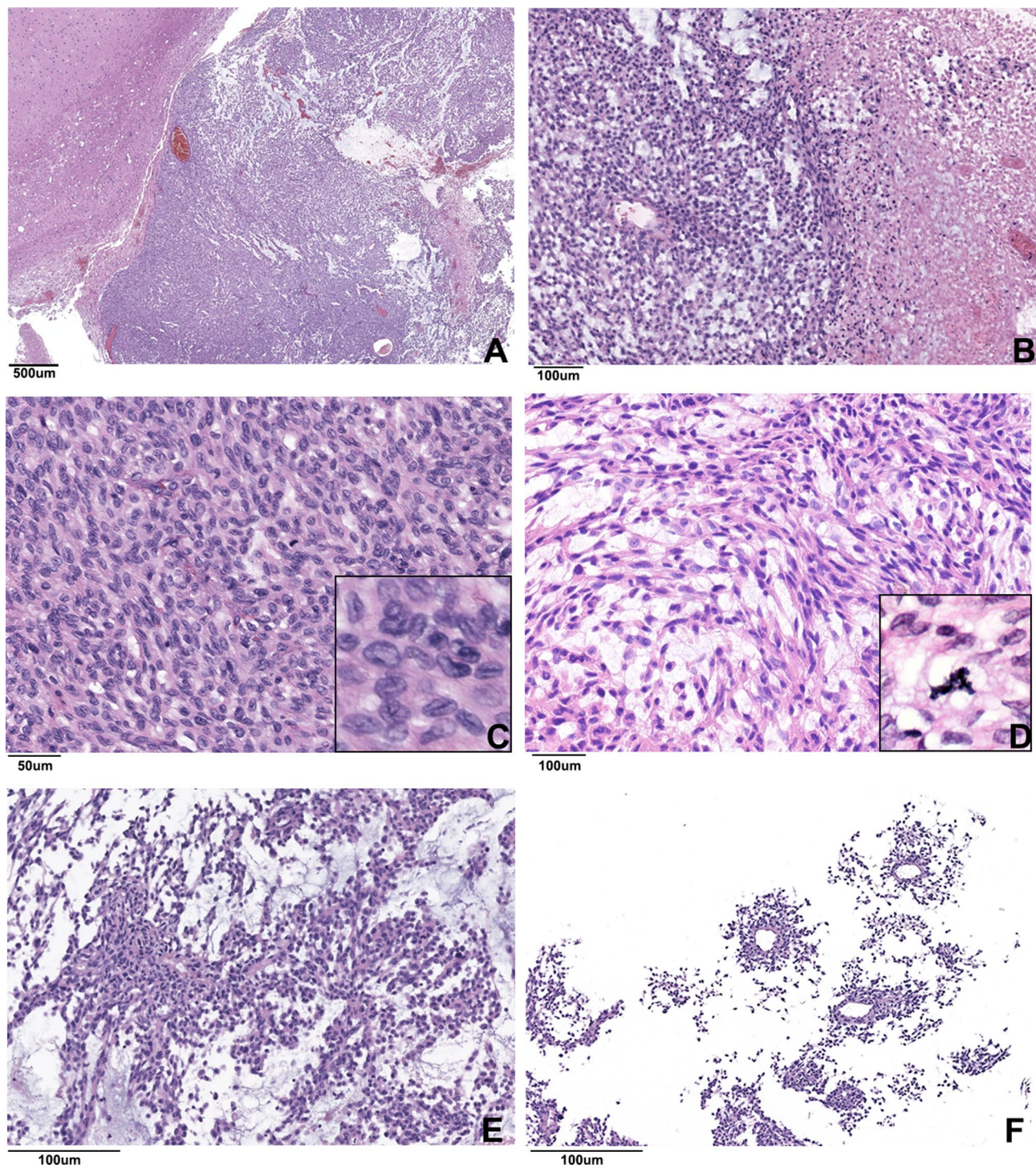


Fig. 3 Histopathological features of the recurrent tumor. The tumor had a clear boundary with the surrounding normal brain tissue (**A**). The tumor cells predominantly exhibited a solid arrangement (**B**), with the solid areas primarily consisting of oval and short-spindle cells (**C**). In certain regions, loosely arranged short-spindle cells were observed (**D**) with a mucinous background noted (**E**). The tumor had high cellular density, significant nuclear atypia with visible nuclear grooves (lower right corner of Fig. 3C), and frequent mitoses (lower right corner of Fig. 3D). Areas of coagulative necrosis were observed (**B**), with a few perivascular pseudorosettes (**F**) at the margins

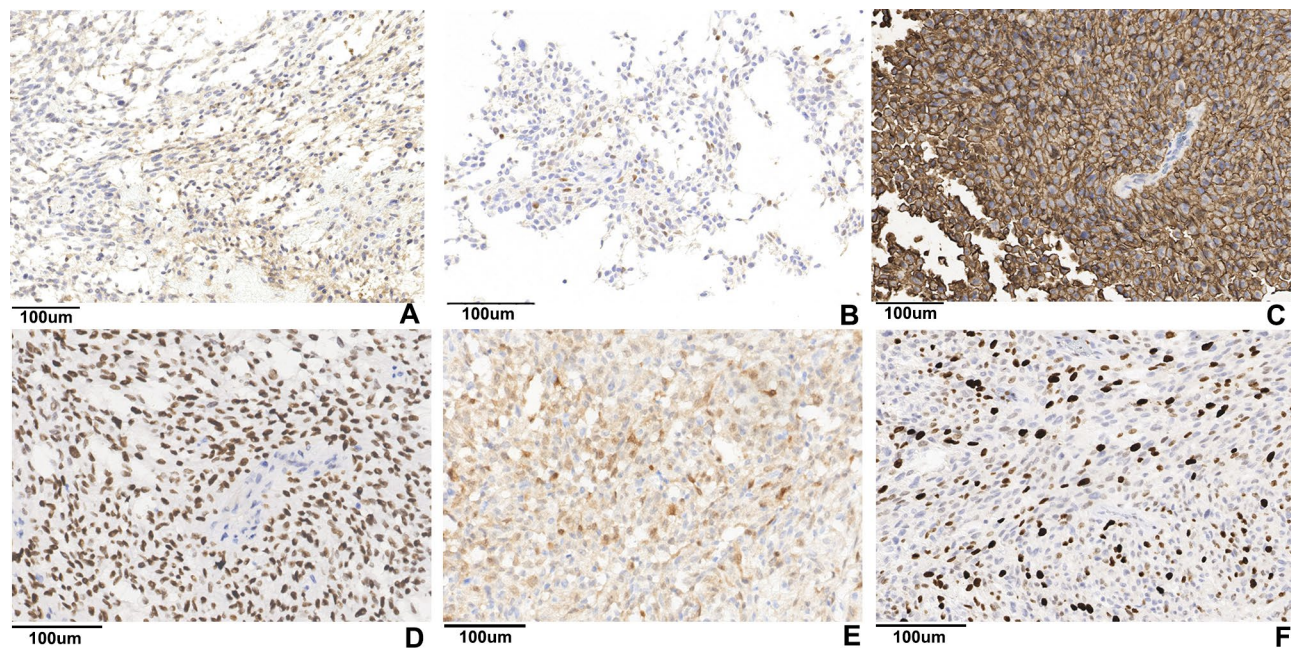


Fig. 4 Immunohistochemical features of the second tumor. A subset tumor cells expressed GFAP (**A**) and OLIG2 (**B**), while most tumor cells EMA showed strong positivity (**C**). The tumor was diffuse positive for SOX2 (**D**) and p16 (**E**). The MIB-1 labelling was 40% (**F**)

By targeted next-generation DNA sequencing, the tumor demonstrated *TCF3* fusion with *BEND2* as the 3' partner, which was validated by reverse transcription polymerase chain reaction (RT-PCR) and Sanger sequencing (Fig. 6B). The primers of RT-PCR were FP: ACCAGCCTCATGCACAAACCA and RP: GGG CACTCGTATTCCCGA. The breakpoint fell within exon 16 in *TCF3* and exon 7 in *BEND2*, resulting in an in-frame fusion. An *MNI* fusion was not detected by

break-apart fluorescent in situ hybridization and DNA sequencing. *ACVR1* c.1112_1113delinsCT (p.G371A), *PDGFRA* c.2315 C>A (p.S772Y), *DDR1* c.2494G>A (p.V832M), *KMT2C* c.962G>A (p.S321N), *CCND1* amplification were detected. No hot-spot mutations in *IDH1*, *IDH2*, *BRAF*, *FGFR1*, *TERT* promoter, *H3F3A* and *HIST1H3B* were detected in sequencing. The integrated diagnosis was high-grade neuroepithelial tumor with *TCF3::BEND2* fusion, not elsewhere classified (NEC).

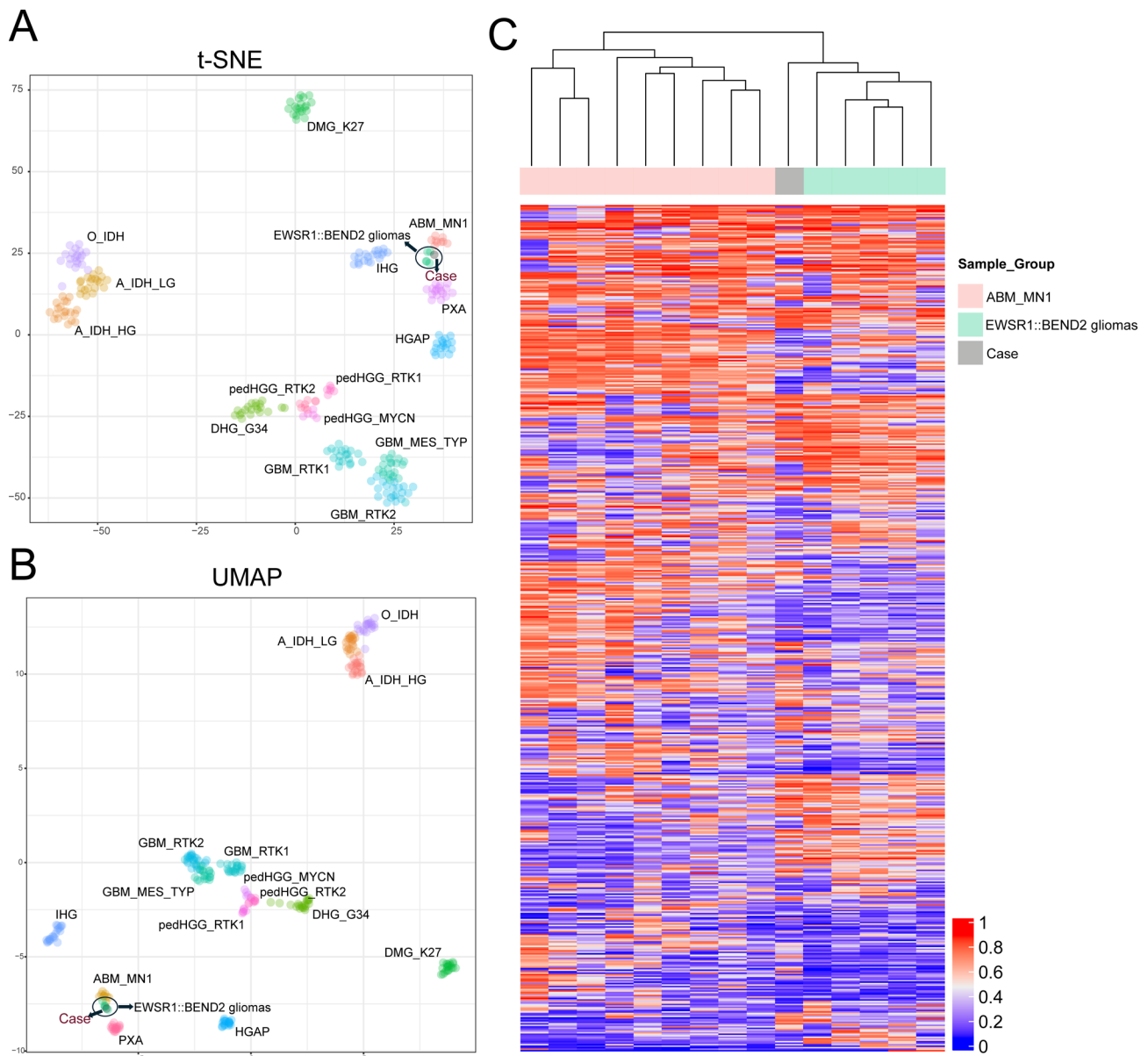


Fig. 5 DNA methylation array analysis. The present case is positioned in close proximity to the *EWSR1::BEND2* gliomas group across both t-SNE (**A**) and UMAP plots (**B**). Unsupervised hierarchical clustering of DNA methylation data from the present case, 5 astroblastoma-like gliomas with *EWSR1::BEND2* fusion and 9 astroblastomas with confirmed *MN1*-altered, with a heatmap of the 20,000 most differentially CpG sites shown (**C**)

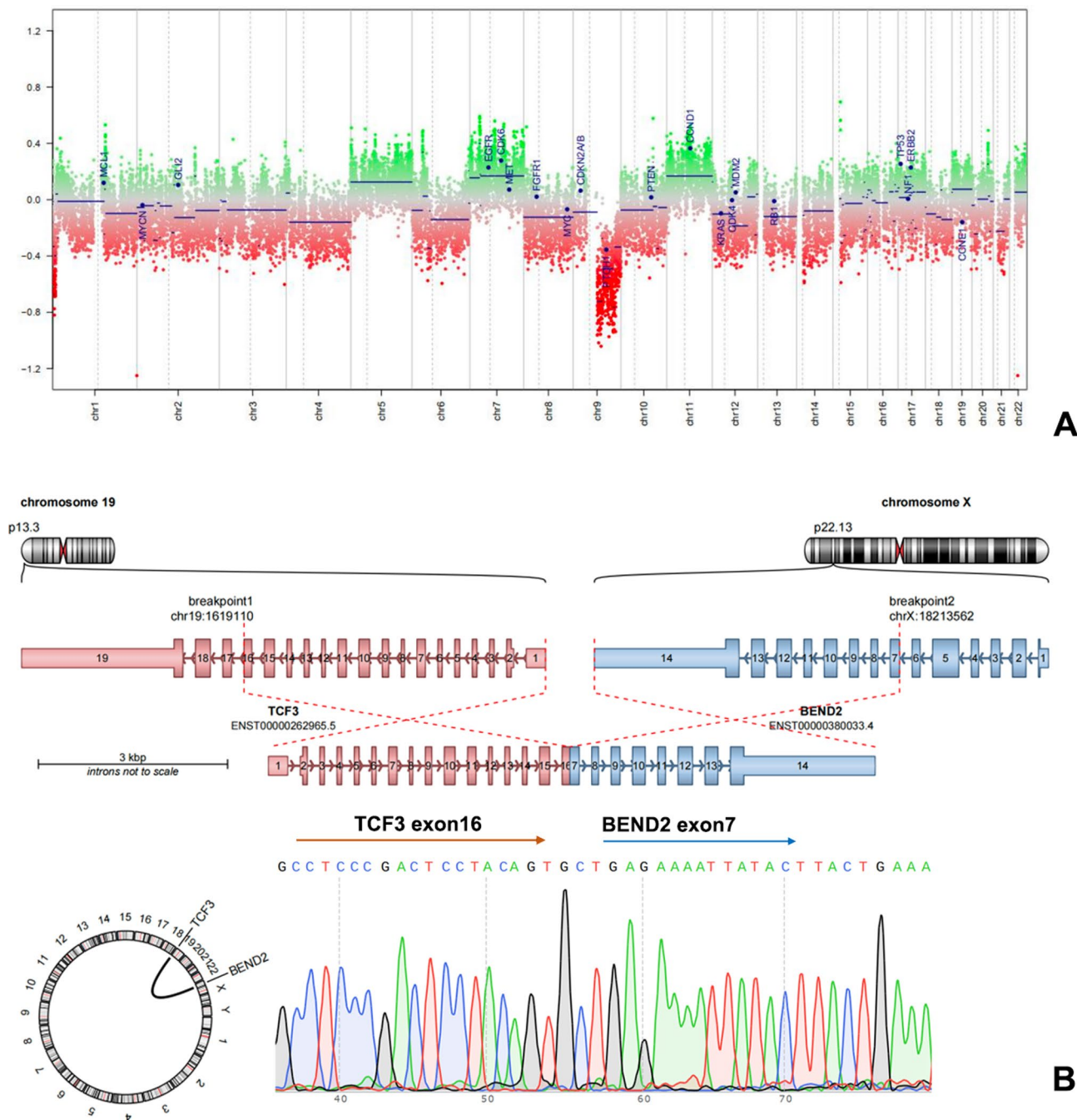


Fig. 6 Copy number variation profile (A). A schematic of the genomic rearrangement resulting in a novel *TCF3::BEND2* gene fusion, validated by RT-PCR (B)

Discussion and conclusion

The 2021 WHO central nervous system (CNS) tumor classification characterizes astroblastoma *MNI*-altered by the *MNI* structural rearrangements, most commonly fusing with the *BEND2* gene (*MNI::BEND2*) and sometimes with *CXXC5* (*MNI::CXXC5*). Astroblastoma with *MNI*-altered typically occurred in girls and mainly supratentorial. The tumor reported here shows many similarities with astroblastoma *MNI*-altered cases including

young female patient and hemispheric location. However, there are notable differences. The present tumor shows significant mucinous degeneration and lacks the typical astroblastoma-like pseudorosette of astroblastoma *MNI*-altered. Immunophenotypically, astroblastomas typically express GFAP, OLIG2, and EMA to varying extents. In this present case, only a few tumor cells expressed GFAP and OLIG2, while most tumor cells EMA showed aberrant strong positivity. Astroblastoma *MNI*-altered often

shows recurrent mutations in genes like *ABCC1*, *IGF2*, *ABCF1*, and *MSH3* [2]. None of these mutations was found in the present case. Interestingly, this case with *TCF3::BEND2* fusion shared some mutated genes with pediatric-type diffuse high-grade gliomas with H3 mutation. For instance, *ACVR1* mutations, found in 25% of diffuse midline gliomas with H3 K27 alterations [6], and *PDGFRα* mutations, occurring in 50% of diffuse hemispheric gliomas with H3 G34 mutations [7]. Besides, *DDR1* mutation is reported in 11.2% of schwannomas [8].

Recently, a group of astroblastoma-like tumors classified by methylation profiling without *MN1* alteration has been reported, including 11 *EWSR1::BEND2* fused cases, two *MAML1::BEND2* fused cases and one *YAP1::BEND2* fused case [3, 4, 9–13]. The group of *EWSR1::BEND2* fused cases is strikingly enriched for non-hemispheric cases, involving the brainstem (two cases) [4, 11] and the spinal cord (seven cases) [3, 4, 10, 12, 13]. Gliomas harbouring *EWSR1::BEND2* have been reported that they defined an epigenetically distinct subtype of astroblastoma [3, 4]. The current case with *TCF3::BEND2* fusion showed similar DNA methylation profile and poor survival with *EWSR1::BEND2* fused cases but located in cerebral hemisphere. All these astroblastoma-like tumors without *MN1* alteration show same *BEND2* gene as 3' fusion partner. *BEND2* maps to the short arm of the X chromosome (Xp22.13) and encodes a protein characterized by two DNA binding BEN domains. *BEND2* is thus potentially involved in transcription and chromatin regulation [14]. It may be hypothesized that *BEND2* makes more contribution to the biology of astroblastomas relevant compared to *MN1*.

Except astroblastoma, *BEND2* fusion is reported in three sarcomas with two *EWSR1::BEND2* fusions [15, 16] and one *MN1::BEND2* fusion [17]. According to Akihiko et al., DNA methylation profiling revealed that sarcoma with *MN1::BEND2* fusion was plotted close to “Sarcoma (MPNST-like)” using tSNE analysis [17]. We also compared the DNA methylation data of this case with sarcomas. The tumor with *TCF3::BEND2* demonstrated a calibrated score below 0.1 and could not be classified into any of the existing categories for sarcomas. It was plotted close to “plexiform neurofibroma (NFB-PLEX)” and different from sarcoma with *MN1::BEND2* fusion. Given that the present tumor shows no phenotypic resemblance with NFB-PLEX, we prefer to classify it as glioma rather than sarcoma.

Rearrangements involving the *TCF3* gene region (19p13.3) are common in both pediatric and adult B-lymphoblastic leukemia/lymphoma (B-ALL/LBL). The *PBX1* gene (1q23) is the most common translocation partner for *TCF3*, resulting in *TCF3::PBX1* fusion [18]. Based on histological morphology and immunohistochemistry

results, the present case is not considered to be a B-ALL/LBL.

In summary, this is the first report of a novel *TCF3::BEND2* fusion detected in primary intracranial neoplasm. Although an *MN1* alteration and typical morphology of astroblastoma were not detected, the tumor was classified as *EWSR1::BEND2* glioma via the methylation classifier. We provisionally diagnose it as a “high-grade neuroepithelial tumor with *TCF3::BEND2* fusion, NEC”, which may later be classified as astroblastoma. This case broadens the genetic spectrum of tumor with *BEND2*-altered and suggests that *BEND2* alterations may serve as critical determinants for this tumor subgroup within the methylation classifier.

Abbreviations

B-ALL/LBL	B-lymphoblastic leukemia/lymphoma
BEND2	BEN Domain Containing 2
CNS	Rare central nervous system
HGNET-MN1	High-grade neuroepithelial tumor with <i>MN1</i> alteration
MGMT	O6-methylguanine methyl transferase
NEC	Not elsewhere classified
NFB-PLEX	Plexiform neurofibroma
RT-PCR	Reverse transcription polymerase chain reaction
t-SNE	T-distributed stochastic neighbor embedding
TCF3	Transcription Factor 3

Acknowledgements

We gratefully acknowledge Dr. Yun Pan and Dr. Zhengjin Li from the First Affiliated Hospital of Dali University for providing the pathological data from the patients' initial tumors. We also thank Huayin medical company (Guangzhou, China) for their assistance with the data analysis.

Author contributions

Clinical data collection and analysis: LZ, MZ, XW and QY. DNA methylation array analysis: TL. Conducted the molecular studies: LZ, JX and XP. Pathology diagnosis: QZ and NC. Manuscript writing: LZ and NC.

Funding

The authors are supported by the National Natural Science Foundation of China (82273047, 82273073, 82203280) and Science and Technology Support Program of Sichuan Province (2024YFHZ0054).

Data availability

No datasets were generated or analysed during the current study.

Declarations

Ethics approval and consent to participate

This study was approved by Clinical Ethics Committee of West China Hospital of Sichuan University and patient gave consent.

Consent for publication

Not applicable.

Competing interests

The authors declare no competing interests.

Received: 15 August 2024 / Accepted: 2 November 2024

Published online: 11 November 2024

References

- WHO Classification of Tumours Editorial Board (2021) Central nervous system tumoursLyon (France). International Agency for Research on Cancer

2. Lehman NL, Spassky N, Sak M, Webb A, Zumbar CT, Usualieva A et al (2022) Astroblastomas exhibit radial glia stem cell lineages and differential expression of imprinted and X-inactivation escape genes. *Nat Commun* 13(1):p2083. <https://doi.org/10.1038/s41467-022-29302-8>
3. Fu L, Lao IW, Huang L, Ou L, Yuan L, Li Z et al (2024) Spinal cord Astroblastoma with EWSR1-BEND2 Fusion in female patients: a report of four cases from China and a Comprehensive Literature Review. *Am J Surg Pathol*. <https://doi.org/10.1097/PAS.0000000000002298>
4. Lucas CG, Gupta R, Wu J, Shah K, Ravindranathan A, Barreto J et al (2022) EWSR1-BEND2 fusion defines an epigenetically distinct subtype of astroblastoma. *Acta Neuropathol* 143(1):109–113. <https://doi.org/10.1007/s00401-021-02388-y>
5. Aryee MJ, Jaffe AE, Corrado-Bravo H, Ladd-Acosta C, Feinberg AP, Hansen KD et al (2014) Minfi: a flexible and comprehensive Bioconductor package for the analysis of Infinium DNA methylation microarrays. *Bioinformatics* 30(10):1363–1369. <https://doi.org/10.1093/bioinformatics/btu049>
6. Hoeman CM, Cordero FJ, Hu G, Misuraca K, Romero MM, Cardona HJ et al (2019) ACVR1 R206H cooperates with H3.1K27M in promoting diffuse intrinsic pontine glioma pathogenesis. *Nat Commun* 10(1):1023. <https://doi.org/10.1038/s41467-019-08823-9>
7. Chen CCL, Deshmukh S, Jessa S, Hadjadj D, Lisi V, Andrade AF et al (2020) Histone H3.3G34-Mutant Interneuron progenitors co-opt PDGFRA for Gliogenesis. *Cell* 183(6):1617–1633e22. <https://doi.org/10.1016/j.cell.2020.11.012>
8. Agnihotri S, Jalali S, Wilson MR, Danesh A, Li M, Kironomos G et al (2016) The genomic landscape of schwannoma. *Nat Genet* 48(11):1339–1348. <https://doi.org/10.1038/ng.3688>
9. Cuoco JA, Williams S, Klein BJ, Borowicz VM, Ho H, Stump MS et al (2024) Astroblastoma with a Novel YAP1:BEND2 Fusion: a Case Report. *J Pediatr Hematol Oncol* 46(5):e313–e316. <https://doi.org/10.1097/mph.00000000000002885>
10. Rossi S, Barresi S, Colafati GS, Giovannoni I, Miele E, Alesi V et al (2022) Paediatric astroblastoma-like neuroepithelial tumour of the spinal cord with a MAML1-BEND2 rearrangement. *Neuropathol Appl Neurobiol* 48(5):e12814. <https://doi.org/10.1111/nan.12814>
11. Smith-Cohn MA, Abdullaev Z, Aldape KD, Quezado M, Rosenblum MK, Vanderbilt CM et al (2021) Molecular clarification of brainstem astroblastoma with EWSR1-BEND2 fusion in a 38-year-old man. *Free Neuropathol* 2. <https://doi.org/10.17879/freeneuropathology-2021-3334>
12. Walker EN, Laws MT, Cozzi F, Quezado M, Brown DA, Burton EC (2023) A case of disseminated spinal astroblastoma harboring a MAML1::BEND2 fusion. <https://doi.org/10.1111/neup.12960>. *Neuropathology*
13. Yamasaki K, Nakano Y, Nobusawa S, Okuhiro Y, Fukushima H, Inoue T et al (2020) Spinal cord astroblastoma with an EWSR1-BEND2 fusion classified as a high-grade neuroepithelial tumour with MN1 alteration. *Neuropathol Appl Neurobiol* 46(2):190–193. <https://doi.org/10.1111/nan.12593>
14. Dai Q, Ren A, Westholm JO, Duan H, Patel DJ, Lai EC (2015) Common and distinct DNA-binding and regulatory activities of the BEN-solo transcription factor family. *Genes Dev* 29(1):48–62. <https://doi.org/10.1101/gad.252122.114>
15. Palsgrove DN, Manucha V, Park JY, Bishop JA (2023) A low-grade Sinonasal Sarcoma harboring EWSR1::BEND2: expanding the Differential diagnosis of Sinonasal Spindle Cell Neoplasms. *Head Neck Pathol* 17(2):571–575. <https://doi.org/10.1007/s12105-023-01527-z>
16. Salguero-Aranda C, Di Blasi E, Galan L, Zaldumbide L, Civantos G, Marcilla D et al (2024) Identification of Novel/Rare EWSR1 Fusion partners in undifferentiated mesenchymal neoplasms. *Int J Mol Sci* 25(3). <https://doi.org/10.3390/ijm s25031735>
17. Yoshida A, Satomi K, Kobayashi E, Ryo E, Matsushita Y, Narita Y et al (2022) Soft-tissue sarcoma with MN1-BEND2 fusion: a case report and comparison with astroblastoma. *Genes Chromosomes Cancer* 61(7):427–431. <https://doi.org/10.1002/gcc.23028>
18. Rowsey RA, Smoley SA, Williamson CM, Vasmatzis G, Smadbeck JB, Ning Y et al (2019) Characterization of TCF3 rearrangements in pediatric B-lymphoblastic leukemia/lymphoma by mate-pair sequencing (MPseq) identifies complex genomic rearrangements and a novel TCF3/TEF gene fusion. *Blood Cancer J* 9(10):81. <https://doi.org/10.1038/s41408-019-0239-z>

Publisher's note

Springer Nature remains neutral with regard to jurisdictional claims in published maps and institutional affiliations.